Smart Structures and Systems, *Vol. 24, No. 2 (2019) 223-231*
DOI: https://doi.org/10.12989/sss.2019.24.2.223

Design, modelling and analysis of a new type of IPMC motor

Jakub Kołota*

Faculty of Computing, Poznan University of Technology ul. Piotrowo 3A, 60-965 Poznan, Poland

(Received March 29, 2018, Revised April 9, 2019, Accepted May 10, 2019)

Abstract. The properties of Electroactive Polymer (EAP) materials are attracting the attention of engineers and scientists from many different disciplines. From the point-of-view of robotics, Ionic Polymer Metal Composites (IPMC) belong to the most developed group of the EAP class. To allow effective design of IPMC-actuated mechanisms with large induced strains, it is necessary to have adequate analytical tools for predicting the behavior of IPMC actuators as well as simulating their response as part of prototyping methodologies. This paper presents a novel IPMC motor construction. To simulate the bending behavior that is the dominant phenomenon of motor movement process, a nonlinear model is used. To accomplish the motor design, the IPMC model was identified via a series of experiments. In the proposed model, the curvature output and current transient fields accurately track the measured responses, which is verified by measurements. In this research, a three-dimensional Finite Element Method (FEM) model of the IPMC motor, composed of IPMC actuators, simultaneously determines the mechanical and electrical characteristics of the device and achieves reliable analysis results. The principle of the proposed drive and the output signals are illustrated in this paper. The proposed modelling approach can be used to design a variety of controllers and motors for effective micro-robotic applications, where soft and complex motion are required.

Keywords: Electroactive polymer;IPMC; FEM; motor

1. Introduction

Polymers that change shape or size in response to electrical stimulus are called Electroactive Polymers (EAP). They are classified via the mechanisms responsible for actuation as electronic EAP - which are driven by electric fields or coulomb forces or ionic EAP - which change shape by mobility or diffusion of ions and their conjugated substances Bar-Cohen (2001). Research and development of ionic EAP actuators have produced significant progress in recent years. A lot of research has focused on delivering the feasibility of the industrial application of these materials Yow *et al.* (2011), Lutkenhaus (2016). There are a couple of reasons why the ionic EAPs deserve attention, especially from the robotic engineering field. Firstly, they could provide actuator motion without assistance from complicated hardware controllers. Secondly, the inherent flexibility of polymeric materials can be implemented in many engineering applications such as biomimetic machines or complex-shaped devices.

An Ionic Polymer Metal Composite (IPMC) is an electroactive polymer with structures used in actuator control applications. This active material is a special type of flexible transducer that can be used as both sensor and actuator. IPMC actuators are composed of ionomeric membranes sandwiched between two metal-plated electrodes Zhu *et al.* (2014), Zhao *et al.* (2013). When the material is hydrated, the cations diffuse towards the electrode surface under an applied electric field. Inside the polymer structure, anions are interconnected as clusters, providing channels for the cations to flow towards the electrode. Fig. 1 shows that the ionic flow causes the structure to bend towards the anode. This phenomena is the source of actuation-force generation in IPMCs Bar-Cohen (2001), Newbury (2002), Shahinpoor (2003). Moreover, it can be used for miniaturization due to its simple actuator structure. IPMC has some excellent characteristics for mechatronic applications, compared to other soft polymer actuators, as follows: driven with low voltage, low power consumption, fast response, high force density, mechanically and chemically durable. IPMCs are soft, flexible and can work in wet conditions Khawwaf *et al.* (2016), Bhattacharya *et al.* (2016), Bernat et al. (2017). The control problem is still open for underwater applications Weiyan *et al.* (2016), Whitcomb *et al.* (2000), Waldmann and Richter (2007).

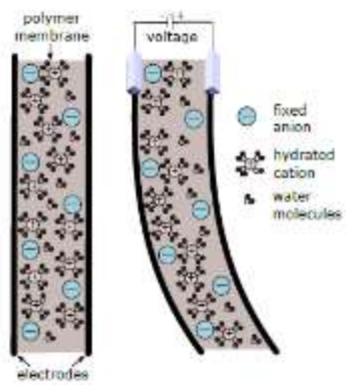

Fig. 1 The working principle of an IPMC actuator

∗Corresponding author, Ph.D.
E-mail: k_kolota@wp.pl

http://www.techno-press.com/journals/sss&subpage=7
ISSN: 1738-1584 (Print), 1738-1991 (Online)

IPMC properties are useful when rapidly shrinking mechanical components, as in robot and machine miniaturization application. In McDaid *et al.* (2010), authors present a novel model for IPMC actuators integrated with a complete mechanical model of the stepper motor. In Kentaro *et al.* (2005) the authors introduce the model of the rotary actuator, which consists of mechanical, electrical and electromechanical dynamics. This paper show that the bending of the ionic polymer could be directly transformed to the limited angle rotation. Various machines that imitate fish, insects or any robot with limbs have been developed Sunkara *et al.* (2016), Shi *et al.* (2013). In Kwang and Tadokoro (2007), the authors suggest that IPMC are good candidates for robotic flapping wings. IPMC materials are promising actuators for portable devices, their unique electrochemical and mechanical properties such as dehydration, hysteresis, and back-relaxation require complex control methods Bernat and Kolota (2016). Research that analyses IPMC materials for control applications are described in McDaid *et al.* (2012), Xing *et al.* (2013), Wang *et al.* (2016), Hao *et al.* (2015), Feng et al. (2016). In Wang *et al.* (2017), the authors propose a double-chamber, valveless pump actuated by a cantilever IPMC, whose deflection is measured by inductive sensors. IPMC-based artificial-muscle controller, designed as a micro-gripper, is described in Jain *et al.* (2013) . This paper uses a simple proof-of-concept IPMC rotary motor as an example. The proposed motor consists of a stator and rotor. The stator is composed of two pairs of IPMC actuators and operates 90 deg out-of-phase, while the rotor comprises of two teeth and no windings. The principle of operation of the drive is like a stepper-motor and is illustrated in detail in the third chapter. The material parameters used in the equivalent-circuit model were experimentally determined. The model was validated by comparing simulated and experimental responses using the transducer modelled in the IPMC rotary motor. This type of device can be implemented in environments where external features are not available for classic drive systems.

2. Model of IPMC actuator

The model development and experimental studies presented in this paper have been carried out on an IPMC kit obtained from Environmental Robots Incorporated. The IPMC consists of a thin (180 μm) polymer membrane with metal electrodes (5 – 10 μm thick) plated on both faces. The surfaces of the plated IPMCs indicate a two-part construction of these materials. Beyond the surface of the membrane, a thicker overlayer of metal is deposited. Optimization of this layer is crucial, as greater thicknesses yield greater surface conductivity, which is needed to charge the membrane and generate the actuative bending. At the same time, greater metal thicknesses increase the composites stiffness, increasing the force required to produce the same displacement.

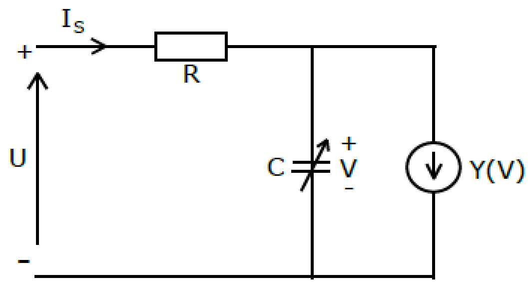

Fig. 2 Equivalent circuit model of Ionic Polymer Metal Composite

2.1 Physical model

IPMC need to be characterized, e.g., their properties and coupling mechanisms need to be understood and modelled, to reach their potential and become accepted in engineering applications. This research considers the nonlinear circuit model developed in Newbury and Leo (2002), Chen *et al.* (2009). Relying on physical phenomena, this model accurately defines nonlinear capacitance $C_1(V)$, virtual capacitance $C_a(V)$ (which describes the electrochemical adsorption process at the polymer-metal interface), ion diffusion resistance Rc, electrode resistance Ra and nonlinear DC resistance of the polymer (expressed as current-voltage relationship Y(V)). Its schema is shown in Fig. 2.

The defined model allows us to develop the following electrochemical dynamics system of equations Chen *et al.* (2009)

$$\frac{dV(t)}{dt} = \frac{U(t) - V(t)}{(R_a + R_c)(C_1(V) + C_a(V))} - \frac{1}{C_1(V) + C_a(V)} Y(V(t)) \tag{1}$$

where U(t) is input voltage and V(t) is electric potential. The current-voltage relationship can be approximated by a series of polynomial functions Y(V(t))

$$Y\big(V(t)\big) = sign\big(V(t)\big)[Y_1|V(t)| + Y_2|V(t)|^2 + Y_3|V(t)|^3]V(t)) \tag{2}$$

where the coefficients Y_1, Y_2, Y_3 can be identified by experiments. The bending moment generated by IPMC actuator is equal to

$$M\big(V(t)\big) = W\alpha_0\kappa_e\left(sign(V(t)2h\sqrt{2\Gamma(|V(t)|)} - V(t)\right) \tag{3}$$

where κ_e is the dielectric constant, h is the thickness, W is the width of IPMC sample and α_0 defines the coupling constant between induced stress and charge density Nemat-Nasser and Li (2000). Function $\Gamma(V(t))$ is given by

$$\Gamma\big(V(t)\big) = \frac{b}{a^2}\left(\frac{aV(t)}{e^{aV(t)} - 1} - ln\left(\frac{aV(t)}{aV(t) - 1}\right) - 1\right) \tag{4}$$

where a and b are the constants defined in Chen *et al*. (2009).

The motion is defined by curvature output y(t) which is proportional to the bending moment Chen *et al*. (2009). However, Newbury (2002), Farinholt (2005) suggests that the mechanical response is attenuated in the high-frequency range. Therefore, we add the additional transfer function. $G(s) = 1/(1 + sT_m)$, to the IPMC model. This results in the following dynamic equation

$$T_m \frac{dy(t)}{dt} + y(t) = \frac{M(V(t))}{Y_e J} \tag{5}$$

where T_m is the time constant, $J = 2/3Wh^3$ is the moment of area inertia and Y_e is the equivalent of Young's modulus of IPMC. The input current is also measurable and is calculated from

$$I_s(t) = \frac{U(t) - V(t)}{R} \tag{6}$$

2.2 Experiments with the IPMC Actuator

We conducted a series of experiments to determine the parameters of the model. The experiment methodology is based on Chen *et al.* (2009). Firstly, we approximate Y(V(t)), considering that the current response under a step voltage input will not vanish at the steady state because of the DC resistance polymer (Fig. 2). The DC current $I_{s\infty}$ flows when the capacitors are fully charged. The approximation of Y(V(t)) is shown in Fig. 4, which suggests that there is good agreement between the model and the experimental data.

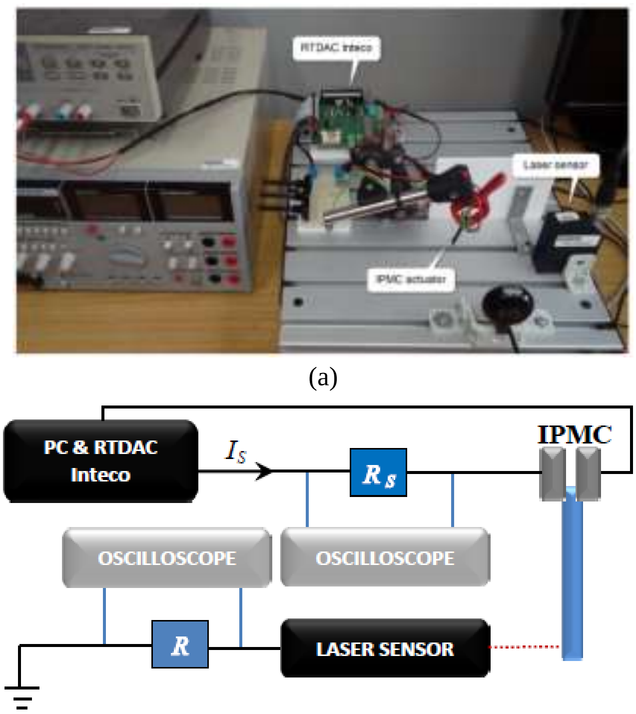

(a)

(b)

Fig. 3 Experimental setup (a) and its schematic diagram (b)

To confirm that the circuit parameters scale correctly for different samples, the results of three experiments were conducted with different IPMC. Table 2 shows the dimensions of the IPMC samples used in the experiments.

To validate the model proposed in this section, as well as material parameters presented in Table 1, simulation results are compared to experimental responses from the same transducer. A time-domain comparison is made using a 1.25 [V] square-wave input voltage signal with a 15[s] period.

Table 1 Parameters in the model

F	R	T	Ra
96487 $\frac{C}{mol}$	8.3143 $\frac{J}{mol \cdot K}$	300 K	15 Ω
R_c	Y_1	Y_2	Y_3
20 Ω	0.02×10^{-3} $\frac{A}{V}$	0.1×10^{-3} $\frac{A}{V}$	0.5×10^{-3} $\frac{A}{V}$
C^{-1}	κ_e	C^{H+}	K_1
1091 $\frac{mol}{m^3}$	53.6×10^{-6} $\frac{F}{m}$	1×10^{-6} $\frac{mol}{m^3}$	8×10^5
α_0	Y_e	q_1	T_m
0.1419 $\frac{J}{C}$	0.62 GPa	0.0105 $\frac{\mu C}{cm^2}$	0.6 s

Table 2 Dimensions of IPMC samples used in experiments

IPMC beam	length [mm]	width [mm]	thickness [μm]
Sample 1	37.0	5.0	180
Sample 2	36.0	5.0	180
Sample 3	33.0	6.5	180

Table 3 Initial current I_{s0} for different samples and series of step voltages

	sample number		
voltage	1	2	3
0.6125 V	35.9 mA	35.6 mA	35.3 mA
1.25 V	70.2 mA	69.6 mA	72.2 mA
2.5 V	140.4 mA	139.2 mA	144.4 mA

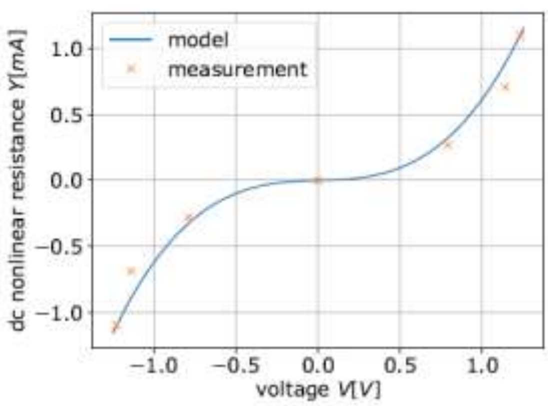

Fig. 4 Nonlinear leakage current in steady state

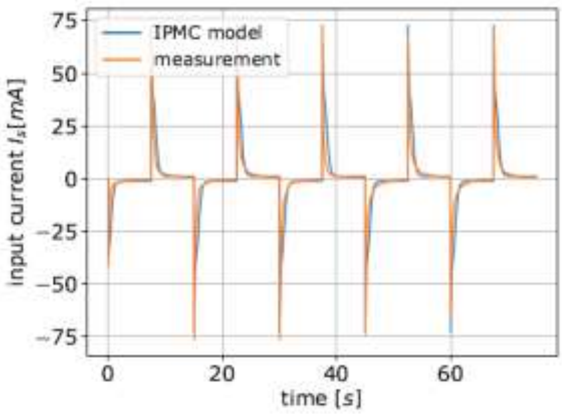

Fig. 5 Current response under step voltage input of 1.25[V]

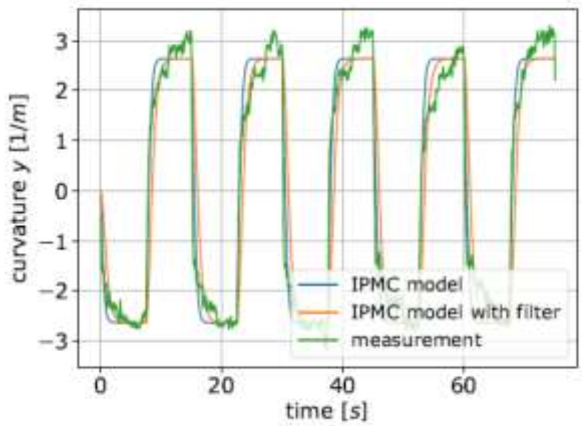

Fig. 6 Curvature output under step voltage input of 1.25 [V]

As a result, the comparison of the current transients shown in Fig. 5 and the curvature output response shown in Fig. 6 validates the model and confirms the quality of the parameters. The responses are shown for two cases: with and without low-pass transfer function. Adding G(s) decreases the mean-square-error by approximately 11%. Furthermore, the current response shows its capacitive potential if switching the voltage generates a current peak, which decays exponentially to some steady state. The curvature output also has an exponential growth rate and above-average noise levels.

To summarize, the IPMC strip can work as actuator and produces a deflection via a voltage excitation. Furthermore, the bending moment of the strip is generated as a function of electric potential. The results obtained in this section confirm that an IPMC can be modelled as simple actuator. In the next section, we apply this single actuator to construct a novel rotary device called a IPMC motor.

3. Polymer motor

In the previous section, we extended our analysis to consider how well the analytic model compares to the measured response of an ionic polymer actuator. To verify the characteristics of the simple actuator, we carried out fundamental experiments. In this section, we demonstrate the qualities of an IPMC motor via a series of experiments. Fig. 7 shows the structure of the proposed motor and its 3D calculation mesh. The dimensions and main parameters of the IPMC motor are defined in Table 4. Four thin IPMC actuators are attached to a stator that is 90 deg out of phase. Their deflection is forced by an external voltage signal, which generates a rotor-like motion that behaves like a stepper motor.

The mechanical simulation of the motor was conducted via Finite Element Method, while the electric circuit, with electromechanical coupling, is modelled via (1) and (3). The simulation schema is presented in Fig. 8 and the input parameters of the mesh are shown in Table 5.

Table 4 Dimensions in the motor model

Motor dimension	Value	Unit
Rotor and stator thickness	7	[mm]
Inner rotor diameter	80	[mm]
Outer rotor diameter	84	[mm]
Rotor tooth height	0.75	[mm]
Rotor tooth length	2	[mm]
Friction coefficient	0.8×10-4	[Nms]

Table 5 Properties of the mesh

Mesh property	Value
Element type	Solid
Element shape	Tetrahedral
Element order	Linear
Edge shape	Straight
Nodes	578
Elements	1479

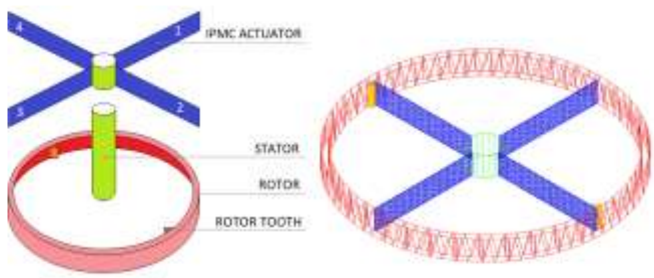

Fig. 7 The structure of IPMC stepper motor (left) and its three-dimensional mesh (right)

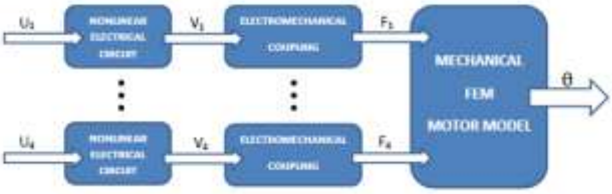

Fig. 8 The simulation schema of IPMC motor

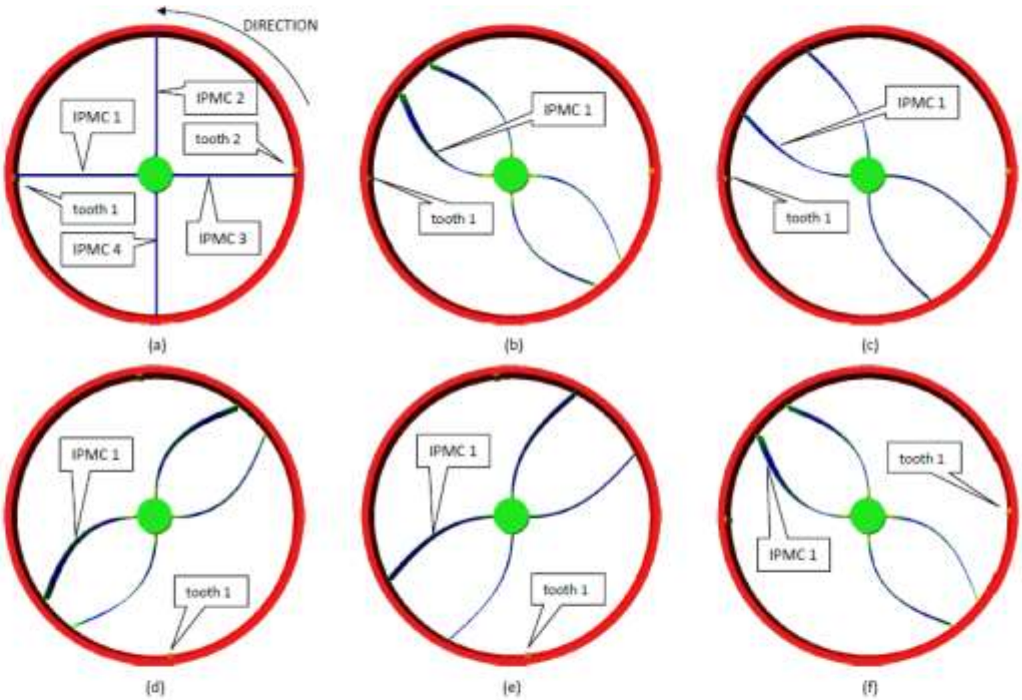

Fig. 9 The working principle of IPMC motor where the first stage is a-c and the second stage is d-f. The following motor steps are illustrated in time: (a) 0[s] (b) 3.1[s] (c) 6.3[s] (d) 9.3[s] (e) 12.5[s] (f) 15.6[s]

3.1 Operating principle

To provide some insight into the principle of motor operation, we shall discuss two stages, which are shown in Figure 9.

1. In the first stage IPMC actuators 1 and 3 touch the rotor tooth and generate torque. At the same time, IPMC actuators 2 and 4 deflect to avoid blocking contact with the rotor tooth.
2. In the second stage IPMC actuators 2 and 4 touch the rotor tooth and generate torque. At the same time, IPMC actuators 1 and 3 deflect to avoid blocking contact with the rotor tooth.

If we alternate between case one and two repeatedly, the rotor will rotate. The time between switching stages describe the motor speed.

The sequence of motor movements of the IPMC presented in Fig. 10 visualizes the moment of pushing the rotor tooth through the actuator 1 and then taking it over the actuator 4. In the same cycle the second tooth is pushed by the actuator 3 and taken by the actuator 2. This stage illustrate the stages between c-e in Fig. 9.

3.2 Motor driver

To design the motor driver, we apply the separation rule, which is a well-known rule for electric motors. Therefore, we design a voltage waveform to run the motor. If the electric motor is symmetric, then the excitation voltage is also designed as symmetric. We propose

$$U_k(t) = Usin\left(\frac{2\pi}{T_s}t + \varphi_k\right) \tag{7}$$

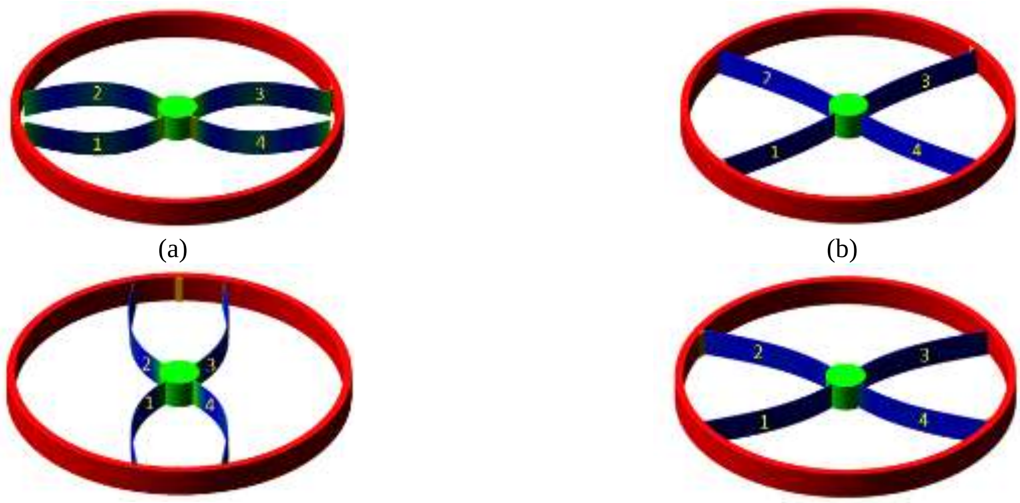

(a) (b)

(c) (d)

Fig. 10 The sequence of the IPMC motor's actuators motions in order to make rotor movement

where k = 1,…, 4 is the phase index, T_s is the time of single stage, $\varphi_1 = \varphi_4 = 0$ deg, and $\varphi_2 = \varphi_3 = 180$ deg are the phase offsets. The voltages shown above are also compatible with the principle of operation described in the previous subsection. The voltage amplitude is set to 1.0[V], and Ts is equal to 12.5[s]. Furthermore, the voltage amplitude is found to generate enough torque to overcome the rotors inertia and friction. The proposed voltage waveform was applied to the FEM model of the motor because it is visible in Fig. 8. As a result, we obtain the rotor angle position. Additionally, we get an IPMC actuator deflection, which is expressed as the curvature output

$$y(t) = \frac{d(t)}{L^2 + d(t)} \tag{8}$$

where y(t) is the curvature output, L is the length of IPMC actuator and d(t) is the deflection in z direction. Fig. 10 shows the curvature output of all IPMC actuators. The output of the curvature waveform is the same, due to symmetry, as the force waveform. The IPMC actuator appears to have nonlinear dynamics, if the curvature output contains high-order frequencies.

Furthermore, we also calculate the torque acting on a rotor, hence we know the rotor speed and position. Fig. 11 shows the rotor position. The figure also suggests that the rotor has 90 deg steps. If the switches are slow, then the motor will have quasi-stationary motion, like a stepper motor Bernat *et al.* (2013). It is possible to decrease the time step T_s, and hence, to increase the rotor speed.

3.3 Feedback possibilities and hardware extensions

In the previous subsection, the rotor motion is caused by a time-dependent force signal. This mode is an open loop, if we do not apply information from rotor position. Stepper motors are typically open loop models Bernat *et al.* (2014). In the proposed motor concept, a closed loop form may also be used. In such modes, we should measure rotor position. The most accurate model adds an encoder to the rotor shaft. There is also a possibility to work with only simple configurations or those considering optics barriers. The key point is to track the first tooth in the rotor when it is in the middle of IPMC actuators 1 and 2, and the second tooth is in the middle of IPMC actuators 3 and 4.

The geometry shown in Fig. 7 is the simplest motor configuration that can achieve motion. Alternate motor configurations can be designed to produce more torque or smoother motion. The first possibility is to add more IPMC actuators and rotor teeth. This will increase the resolution of the motor steps. The second possibility is to join two motors with an offset. For example, in the case of 2 stacked motors, the offset is 45 deg, for 3 stacked motors the offset is 30 deg and for 4 stacked motor, the offset is 22.5 deg. The last configuration is shown in Fig. 12.

3.4 Features

To summarize the motor construction, we discuss its the main features. If an IPMC actuator is working in a hydrated environment, the motor can do well. This allows the motor to work while completely immersed. Operating in water is an advantage of the polymer motor, when compared to standard electric motors, which generally do not work in liquid. Another interesting property is the capacitive potential of the motor. This suggests that the current is lowest at the steady state, which is not the case for electric windings with inductive potentials. This, in turn, can decrease the power of the electric circuit and reduce motor overheating. Furthermore, the flexible construction of IPMC actuators and rubber rotors enable the deflection of a rotor. Thus, IPMC actuators can be applied to robotic applications, for instance the flexible robotic wheel. Another possibility is to build asymmetric construction with different length actuators. The motor retains the good properties of IPMC actuators which include anticorrosion/antistatic properties, high number of working about 106 cycles, and miniaturization properties.

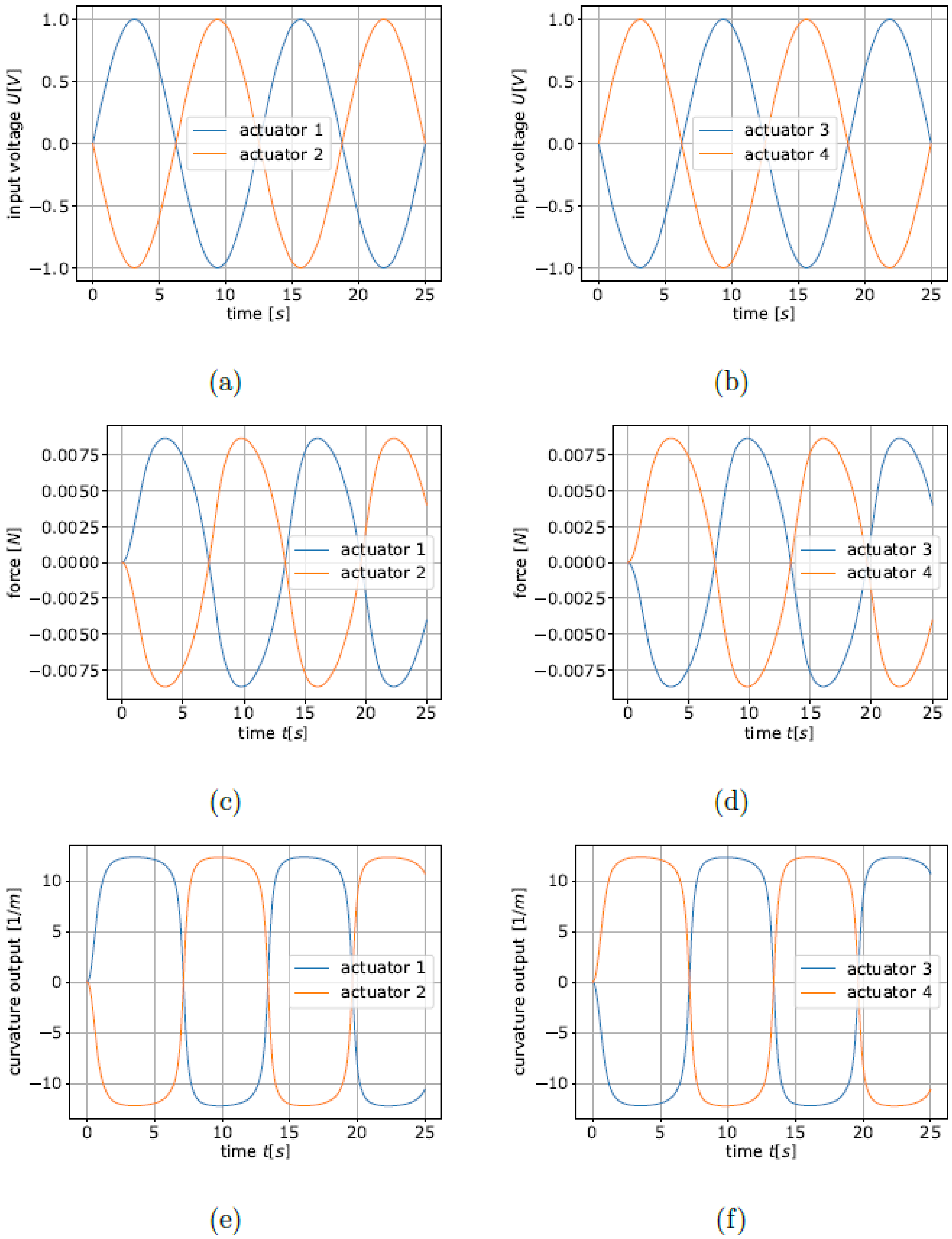

Fig. 11 The input voltage of IPMC actuators (a) 1 and 2, (b) 3 and 4. The force of IPMC actuators: (c) 1 and 2, (d) 3 and 4. The calculated curvature output: (e) 1 and 2, (f) 3 and 4

The experiments have shown that IPMC actuators can support dynamic micro-manipulation strategies of robotic systems. In a real drive, the rotor can be embedded in various ways. One of the possible applications of the proposed motor is to place rotor between gear transmissions. Another conception may be to transmit the driving force through a torsion bolt. Both solutions are presented in Fig. 13.

5. Conclusions

IPMC actuators are extremely important for advanced applications of robotic systems. Conventional motors may not meet characteristic requirements like flexibility or being lightweight. They can be configured into complex shapes and their properties can be tailored according to demand. Therefore, this device is safer than conventional devices in wet environments.

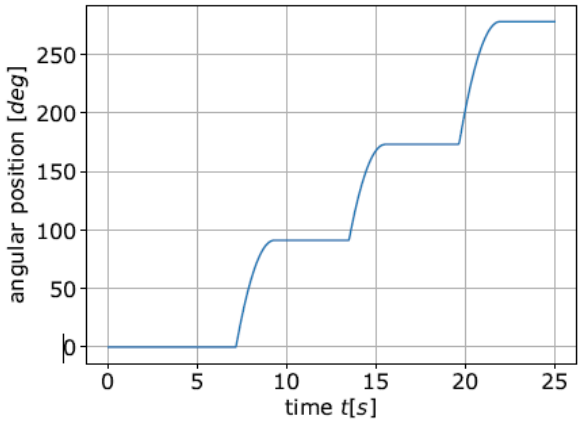

Fig. 12 The curvature output of IPMC actuators

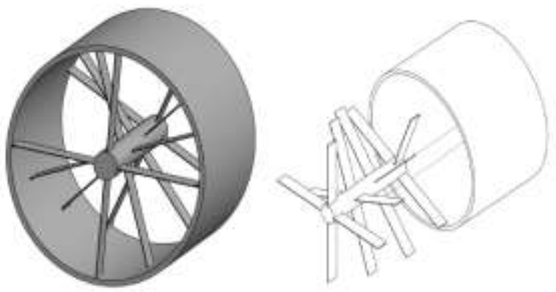
Fig. 13 The curvature output of IPMC actuators

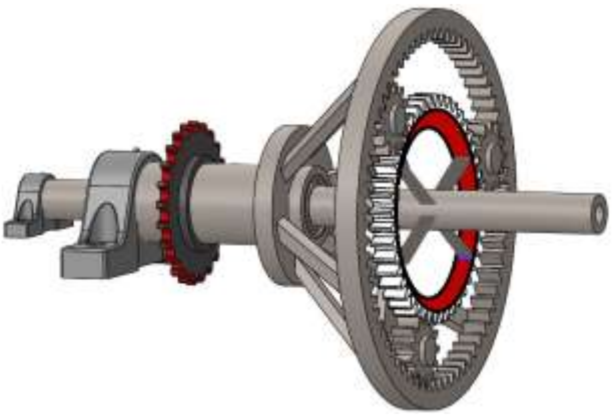
Fig. 14 Examples drive systems using an IPMC motor

In this paper, we describe unique devices as a novel concept of the IPMC motor. Experiments have shown that IPMC actuators can support dynamic micro-manipulation strategies. We also described a nonlinear model of the IPMC actuator, which is the basis of the new device. This model was verified via experiments and the finite-element approach is used for the dynamic modelling of a novel motor construction. The proposed motor structure can be a possible solution for effective underwater micro-machines and other robotics applications where soft and complex motion are required. Promising advances in IPMC indicate that this material could be an enabling technology in the creation of new types of motors. At the most basic level, IPMC motors may be substituted for an existing electromagnetic device in an otherwise classical system architecture that can provide many benefits: physical layout, mass, flexibility and robot control systems. The modelling effort in this work has demonstrated that IPMC transducers can be accurately used towards new kinds of rotary motors.

References

Bar-Cohen, Y. (2001), Electroactive polymer (EAP) actuators as artificial muscles: reality, potential, and challenges, SPIE Press, Bellingham, WA, USA.

Bernat, J. and Kolota, J. (2016), "Sensorless position estimator applied to nonlinear IPMC model", *Smart Mater. Struct.*, **25** (11), 115037.

Bernat, J., Kolota, J. and Stepien, S. (2017), "SDRE controller considering multi observer applied to nonlinear ipmc model", *Smart Struct. Syst.*, **20**(1), 1-10. https://doi.org/10.12989/sss.2017.20.1.001.

Bernat, J., Kolota, J. and Stepien, S. (2013), "The fem analysis of electromagnetic torque of hybrid stepper motor with different load", *Electrical Review*, **89**(7), 186-189.

Bernat, J., Kolota, J., Stepien, S. and Szymanski, G. (2014), "Adaptive control of permanent magnet synchronous motor with constrained reference current exploiting backstepping methodology", *Proceedings of the IEEE Conference on Control Applications (CCA)*, Juan Les Antibes, France, October.

Bhattacharya, S., Bepari, B. and Bhaumik, S. (2016), "Soft robotic finger fabrication with pdms and ipmc actuator for gripping", SAI Computing Conference (SAI), London, UK, July.

Chen, Z., Hedgepeth, D.R. and Tan, X. (2009), "A nonlinear, control-oriented model for ionic polymer-metal composite actuators", *Smart Mater. Struct*., **18**(5), 055008.

Farinholt, K.M. (2005), "Modeling and characterization of ionic polymer transducers for sensing and actuation", Ph.D. Dissertation, Virginia Polytechnic Institute and State University.

Feng, G.H. and Huang, W.L. (2016), "Investigation on the mechanical and electrical behavior of a tuning fork-shaped ionic polymer metal composite actuator with a continuous water supply mechanism", *Sensors*, **16**(4), Published online. https://doi.org/10.3390/s16040433.

Hao, L., Chen, Y. and Sun, Z. (2015), "The sliding mode control for different shapes and dimensions of IPMC on resisting its creep characteristics", *Smart Mater. Struct*., **24**(4), 045040.

Jain, R.K., Datta, S. and Majumder, S. (2013), "Design and control of an IPMC artificial muscle finger for micro gripper using emg signal", *Mechatronics*, **23**(3), 381-394. https://doi.org/10.1016/j.mechatronics.2013.02.008.

Kentaro, T., Zhi, W.L., Kinji, A., and Kenji, T., "Limited-angle motor using ionic polymer-metal composite", Proc. SPIE 5759, Smart Structures and Materials 2005: Electroactive Polymer Actuators and Devices (EAPAD), (6 May 2005); doi: 10.1117/12.599503;

Khawwaf, J., Zheng, J., Al-Cihanimi, A., Man Z, and Nagarajah, R. (2016), "Modeling and tracking control of an ipmc actuator for underwater applications", *Proceedings of the International Conference on Advanced Mechatronic Systems (ICAMechS), Melbourne*, Australia, November.

Kwang, J.K. and Tadokoro, S. (2007), Electroactive polymers for robotics applications, Artificial muscles and sensors, Springer-Verlag, London.

Lutkenhaus, J. (2016), "Electroactive polymers as battery electrodes", *TechConnect Briefs*, **2**, 39-41.

McDaid, A.J., Aw, K.C., Haemmerle, E. and Xie, S.Q. (2012), "Control of ipmc actuators for microfluidics with adaptive "online" iterative feedback tuning", *IEEE/ASME T. Mechatron*., **17**(4), 789-797. DOI: 10.1109/TMECH.2011.2135373.

McDaid, A., Aw, A.C., Patel, K., Xie, S. and Haemmerle, E. (2010), "Development of an ionic polymer-metal composite stepper motor using a novel actuator model", *Smart Nano Mater*., **1**(4), 261-277. https://doi.org/10.1080/19475411.2010.523123.

Nemat-Nasser, S. and Li, J. (2000), "Electromechanical response of ionic polymer-metal composites", *J. Appl. Phys*., **87**(7), 3321-3331. https://doi.org/10.1063/1.372343.

Newbury, K. (2002), "Characterization, Modeling, and Control of Ionic Polymer Transducers", Ph.D. Dissertation, Virginia Polytechnic Institute and State University, Virginia.

Newbury, K.M. and Leo, D.J. (2002), "Electromechanical modeling and characterization of ionic polymer benders", *J. Intel. Mat. Syst. Str*., **13**(1), 51-60. https://doi.org/10.1177/1045389X02013001978.

Shahinpoor, M. (2003), "Ionic polymer-conductor composites as biomimetic sensors, robotic actuators and artificial muscles - a review", *Electrochimica Acta*, **48**(14-16), 2343-2353. https://doi.org/10.1016/S0013-4686(03)00224-X.

Shi, L., He, Y., Guo, S., Kudo, H., Li, M. and Asaka K. (2013), "IPMC actuator-based a movable robotic venus flytrap", *Proceedings of the ICME International Conference on Complex Medical Engineering*, Beijing, China, May.

Sunkara, V., Ye, Z., Chakravarthy, A. and Chen, Z. (2016), "Collision avoidance by ipmc actuated robotic fish using the collision cone approach", *Proceedings of the 2016 IEEE International Conference on Simulation, Modeling, and Programming for Autonomous Robots (SIMPAR)*, San Francisco, CA, USA, December.

Waldmann, C. and Richter, L. (2007), "Traction properties of the wheels of an underwater crawler on different soils", *Proceedings of the Oceans Conference Record (IEEE)*, Vancouver, BC, Canada, September.

Wang, H., Chen, J., Lau, H. and Ren, H. (2016), "Motion planning based on learning from demonstration for multiple-segment flexible soft robots actuated by electroactive polymers", *IEEE Robot. Automat. Lett*., **1**(1), 391-398. DOI: 10.1109/LRA.2016.2521384.

Wang, J., McDaid, A.J., Lu, C.Z. and Aw K.C. (2017), "A compact ionic polymer-metal composite (IPMC) actuated valveless pump for drug delivery", *IEEE/ASME T. Mechatron*., **22**(1), 196-205. DOI: 10.1109/TMECH.2016.2624762.

Weiyan, S., Canjun, Y. and Faju, Q. (2016), "Analysis on the steering characteristics of an underwater exploration robot", *Proceedings of the IEEE/ASME International Conference on Advanced Intelligent Mechatronics (AIM)*, Banff, AB, Canada, September.

Whitcomb, L., Yoerger, D., Singh, H. and Howland, J. (2000), "Advances in underwater robot vehicles for deep ocean exploration: Navigation, control, and survey operations", in: (Eds., Hollerbach J.M. and Koditschek D.E.), Robotics Research, Springer, London.

Zhao, Y., Xu, B., Zheng, G., Zheng, J., Qiu, X., Zhuang, M. and Sun, D. (2013), "Improving the performance of IPMCs with a gradient in thickness", *Smart Mater. Struct*., **22**(11), 115035.

Zhu, Z., Chang, L., Asaka, K., Wang, Y., Chen, H., Zhao, H. and Li, D. (2014), "Comparative experimental investigation on the actuation mechanism of ionic polymer-metal composites with different backbones and water contents", *J. Appl. Phys*., **115**, 124903. https://doi.org/10.1063/1.4869537.

Xing, H.L., Jeon, J.H., Park, K.C. and Oh I.K. (2013), "Active disturbance rejection control for precise position tracking of ionic polymermetal composite actuators", *IEEE/ASME T. Mechatron*., **18**(1), 86-95. DOI: 10.1109/TMECH.2011.2163524.

Yow, S.Z., Lim, T.H., Yim, E.K.F., Lim, C.T. and Leong, K.W. (2011), "A 3d electroactive polypyrrole-collagen fibrous scaffold for tissue engineering", *Polymers*, **3**(1), 527-544. https://doi.org/10.3390/polym3010527.

HJ